Supplementary material for "Using Delaunay triangularization to characterize non-affine displacement fields during athermal, quasistatic deformation of amorphous solids"

Weiwei Jin, Amit Datye, Udo D. Schwarz, Mark D. Shattuck, and Corey S. O'Hern

1 Spatio-temporal evolution of the non-affine displacement fields

Supplementary Movie 1, which is available as a separate file, shows the spaito-temporal evolution of the von Mises strain ε_α^{vm} of each triangle α (left panel) during the initial quasi-elastic segment (from the thermally quenched zero-strain configuration), as well as the segment in Fig. 3 (a) and (b) of the main text. The von Mises strain of each triangle is obtained by comparing successive configurations separated by $30\delta\gamma$ during each quasi-elastic segment. The color scale from blue to red indicates increasing von Mises strain from 0 to 0.001. The associated non-affine displacement fields are shown in the right panel.

Supplementary Movie 2 shows the spaito-temporal evolution of the von Mises strain ε_α^{vm} of each triangle α (left panel) during the shear stress drop in Fig. 3 (c) of the main text. The von Mises strain of each triangle is obtained by comparing successive images along the minimal energy path of this stress drop. The color scale from blue to red indicates increasing von Mises strain from 0 to 0.002. The associated non-affine displacement field is shown in the middle panel. The shear stress Σ_{xy} and the total potential energy U as a function of the image index are presented in the right panel. A vertical blue line tracks the evolution of the image index in the left and middle panels.

2 Correlations between high-strain regions

There are strong correlations between localized high-strain regions at the end of quasi-elastic segments and the *first* high-strain region that occurs during the corresponding stress drops, but not subsequent high-strain regions that form. To quantify these correlations, we identify the disk region (with radius $5.5\sigma_{\rm AA}$) surrounding a given triangle with the largest average von Mises strain $\langle\varepsilon^{vm}\rangle_{\rm max}$, where the strain is calculated by comparing successive images during the stress drop or the successive configurations during the quasi-elastic segment, and consider the center of the disk region as the center of the high-strain region. Fig. S1 below shows $\langle\varepsilon^{vm}\rangle_{\rm max}$ for each image during an example stress drop for which three high-strain regions are detected. The high-strain region at the end of the quasi-elastic segment is the same region as that indicated by the first peak in $\langle\varepsilon^{vm}\rangle_{\rm max}$. This high-strain region dissolves (near image 50) and a new one forms, indicated by the second peak in $\langle\varepsilon^{vm}\rangle_{\rm max}$, near image 75. The second high-strain region dissolves (near image 110) and a new one forms, indicated by the third peak in $\langle\varepsilon^{vm}\rangle_{\rm max}$, near image 125. Similar data is found for other stress drops.

In Fig. S2, we calculate the distribution of the center-to-center separations between the position of the high-strain region at the end of each quasi-elastic segment and the positions of the high-strain regions at local maxima in $\langle\varepsilon^{vm}\rangle_{\rm max}$ during the stress drops. The high-strain region at the end of the quasi-elastic segment does not move significantly before it dissolves, i.e., the average separation between the high-strain region at the end of the quasi-elastic segment and the one corresponding to the first peak in $\langle\varepsilon^{vm}\rangle_{\rm max}$ is $\sim 1.5\sigma_{\rm AA}$. After the high-strain region from the quasi-elastic segment dissolves at the beginning of the stress drop, the location of the next high-strain region is randomly distributed throughout the system.

3 Assessment of system-size effects

We carried out simulations containing $N = 3600$, 8100, and 14400 particles. The resulting stress-strain curves for these system sizes are qualitatively similar as shown in Fig. S3. We find that small stress drops are relatively more frequent for larger system sizes, and larger stress drops are relatively less frequent, which causes the average magnitude of the stress drop to decrease as a power-law with increasing system size, $\langle\Delta\Sigma_{xy}\rangle \sim N^{-\lambda}$, where $\lambda \approx 0.7$. However, as shown in Fig. S4 below, the distributions of the stress drops scaled by the average values, $\frac{\Delta\Sigma_{xy}}{\langle\Delta\Sigma_{xy}\rangle}$, are similar for all system sizes studied.

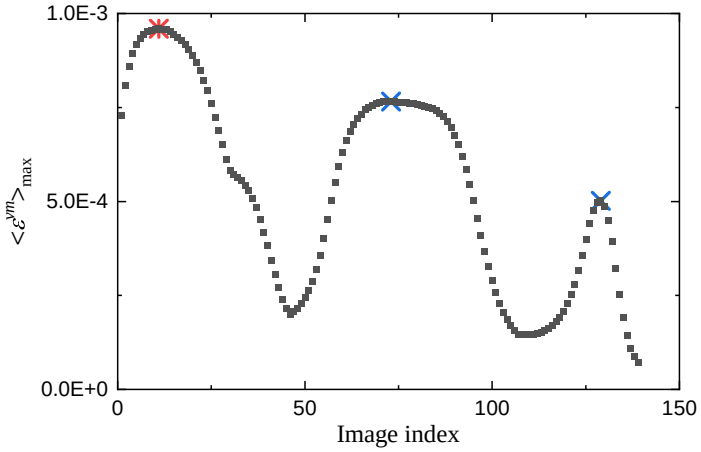

Figure S1: The largest value of the average von Mises strain $\langle\varepsilon^{vm}\rangle_{\max}$ of disk regions (with radius $5.5\sigma_{\rm AA}$) for each image during a typical stress drop. The first maximum in $\langle\varepsilon^{vm}\rangle_{\max}$ (red $*$) corresponds to the high-strain region that occurs at the end of the corresponding quasi-elastic segment. This first high-strain region dissolves and other high-strain regions (blue $\times$'s) form and dissolve during this stress drop.

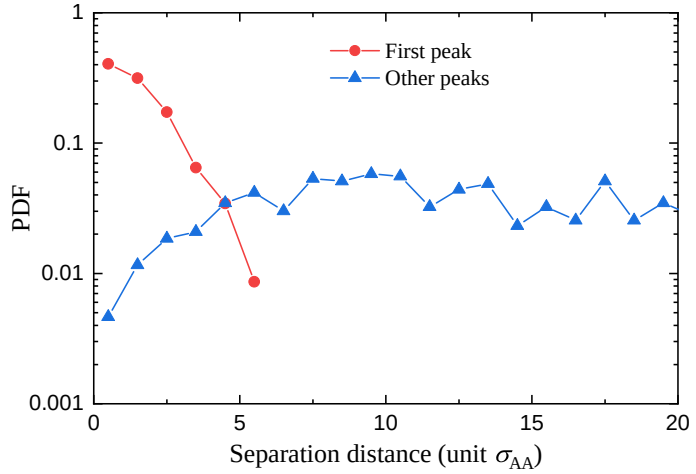

Figure S2: The probability distribution function (PDF) of the center-to-center separations between the high-strain regions at the end of the quasi-elastic segments and those at local maxima in $\langle\varepsilon^{vm}\rangle_{\max}$ (first peak and other peaks) during stress drops. The edge length of the system is $60\sigma_{\rm AA}$.

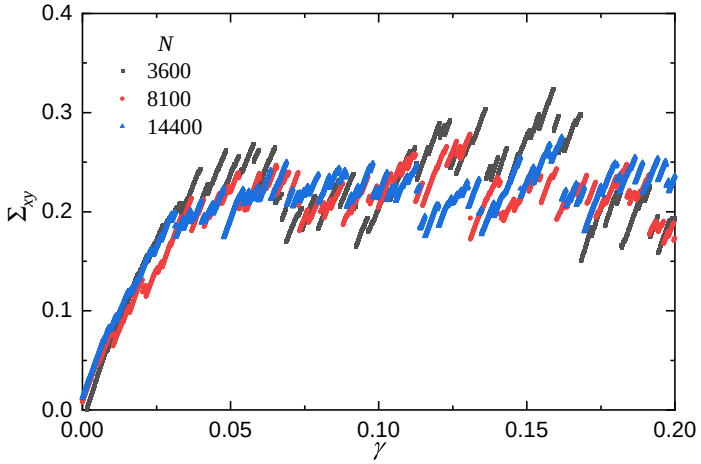

Figure S3: Shear stress Σ_{xy} as a function of shear strain γ for systems with $N = 3600, 8100$, and 14400 particles during athermal, quasistatic simple shear.

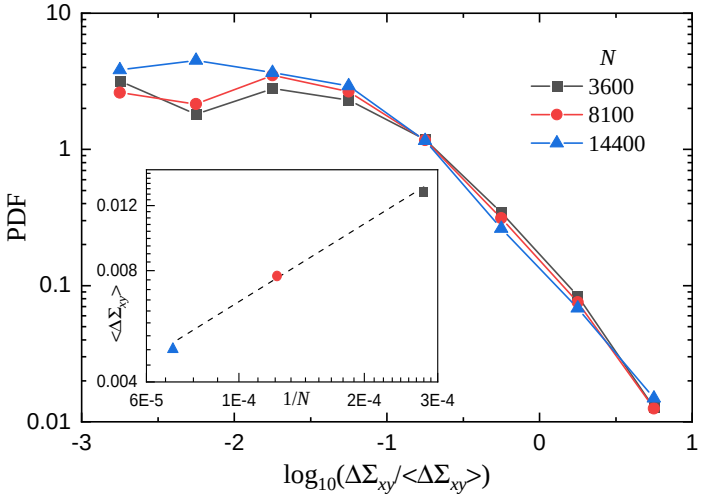

Figure S4: Probability distribution function (PDF) of $\log_{10}(\Delta\Sigma_{xy}/\langle\Delta\Sigma_{xy}\rangle)$, where $\Delta\Sigma_{xy}$ is the absolute value of the stress drop and $\langle\Delta\Sigma_{xy}\rangle$ is the corresponding average value. Inset: The average stress drop $\langle\Delta\Sigma_{xy}\rangle$ plotted as a function of the inverse of the system size $1/N$. The dashed line has slope equal to 0.7.